

Torsional instability of chiral carbon nanotubesD. G. Vercosa,¹ E. B. Barros,^{1,*} A. G. Souza Filho,¹ J. Mendes Filho,¹ Ge. G. Samsonidze,² R. Saito,³ and M. S. Dresselhaus⁴¹*Departamento de Física, Universidade Federal do Ceará, Fortaleza, Ceará, 60455-900, Brazil*²*Department of Physics, Materials Sciences Division, Lawrence Berkeley National Laboratory, University of California at Berkeley, Berkeley, California 94720, USA*³*Department of Physics, Tohoku University, Sendai 980-8578, Japan*⁴*Department of Electrical Engineering and Computer Science and Department of Physics, Massachusetts Institute of Technology, Cambridge, Massachusetts 02139-4307, USA*

(Received 20 January 2010; revised manuscript received 18 March 2010; published 21 April 2010)

In this work we investigate the presence of a torsional instability in single-wall carbon nanotubes which causes small diameter chiral carbon nanotubes to show natural torsion. To obtain insight into the nature of this instability, the natural torsion is calculated using an extended tight-binding model and is found to decrease as the inverse cube of the diameter. The dependence of the natural torsion on chiral angle is found to be different for metallic and semiconducting nanotubes, specially for near-armchair nanotubes, for which the behavior of semiconducting nanotubes deviates from the simple $\sin(6\theta)$ behavior observed for metallic nanotubes. The presence of this natural torsion implies a revision of the calculation of the chiral angle of the nanotubes.

DOI: [10.1103/PhysRevB.81.165430](https://doi.org/10.1103/PhysRevB.81.165430)

PACS number(s): 61.48.De, 78.67.Ch

Several theoretical and experimental studies indicate that the electronic and optical properties of carbon nanotubes are extremely sensitive to structural deformations, such as axial, radial, or torsional strains.¹⁻⁴ Due to the possible applicability of nanotubes for electromechanical actuators, the torsional properties of multiwall and single-wall carbon nanotubes (SWNTs) have been widely investigated both experimentally and theoretically.⁴⁻¹⁰ However, for the interpretation of these works, these reports assume that in their natural state, carbon nanotubes are free from such geometrical deformations. In the case of radial and axial strains, this assumption can always be asserted since these deformations maintain the full symmetry of the nanotube and thus the nanotube structure can be renormalized to the new parameters without losing its basic properties. However, in the case of a torsional strain, the pure translational symmetry of the nanotube is broken and thus the usual symmetry representation of the nanotube unit cell needs to be revised.

One of the main problems involved in the simulation of nanotube properties under torsion is the fact that the application of a torsional stress to the carbon nanotube breaks the pure translational symmetry of the nanotube unit cell. For this reason, calculations involving the effects of torsion are done either on finite-length nanotubes or in supercells. However, these studies were able to obtain important information about the mechanical properties of nanotubes. One interesting result was reported by Liang *et al.*,⁹ which showed that the relationship between the axial-strain-induced torsion in chiral nanotubes is asymmetric with respect to zero strain. On the other hand, Chang *et al.*¹⁰ showed also that the effects of torsion on a chiral single-wall carbon nanotube is dependent on the load direction. These results originate from the fact that chiral nanotubes do not have inversion symmetry and thus the effects of a torsional stress in one direction of a nanotube is different from that in another direction. This fact brings up several different questions, one of which is about the effect of this asymmetry on the nanotube structure itself.

In the present work we investigate the presence of a natural torsion in chiral single-wall carbon nanotubes by using a

symmetry-adapted tight-binding calculation. The presence of this natural torsion is explained in terms of a torsional instability similar to the Peierls instability expected for metallic linear chains. The helical symmetry of the nanotube is taken into consideration by describing the nanotube structure using a helical-angular construction of the nanotube¹¹ and the interactions between the atoms are considered in terms of tight-binding parameters for σ and π orbitals obtained from density-functional theory (DFT) as a function of the interatomic distances.^{12,13} An important work discussing the effect of strain in carbon nanotubes using a helical-symmetry-based first-principles calculation was published by Lawler *et al.*¹⁴ Although, the presence of a natural torsion was not investigated by these authors, it is expected that their method is appropriate for such a study and should be used to verify the simpler model calculations.

Conceptually, SWNTs can be seen as a rolled up graphene sheet. In Fig. 1, the translational primitive cell of a (4,2) nanotube is shown. The chiral vector (\mathbf{C}_h), that lies along the circumferential direction of the tube, defines the tube uniquely. This vector can be written as $\mathbf{C}_h = n\mathbf{a}_1 + m\mathbf{a}_2$ in terms of the primitive vectors of the graphene honeycomb lattice (\mathbf{a}_1 and \mathbf{a}_2), also shown schematically in the figure, and the indexes (n, m) specify the carbon nanotube structure. This unit cell is bounded by the pure rotational symmetry vector \mathbf{C}_h/d , where d is the greatest common divisor of n and m [$d = \text{gcd}(n, m)$], and by the pure translation vector \mathbf{T} .

Figure 1 shows the translation unit cell of a (4,2) SWNT and its structural parameters.¹³ When a torsion is applied to the SWNT, the pure translational symmetry (depicted by the translation vector \mathbf{T} in Fig. 1) is broken. However, the screw translations, such as the one represented by the vector \mathbf{Z} in Fig. 1, remain as symmetry operations of the nanotube. For this reason, it is possible to calculate the electronic properties of torsioned carbon nanotubes by using a helical-angular representation,¹¹ where the electronic states are labeled by a purely rotational quantum number μ , which is related to an angular momentum around the nanotube axis, and a helical quantum number h , which can be loosely related to a linear

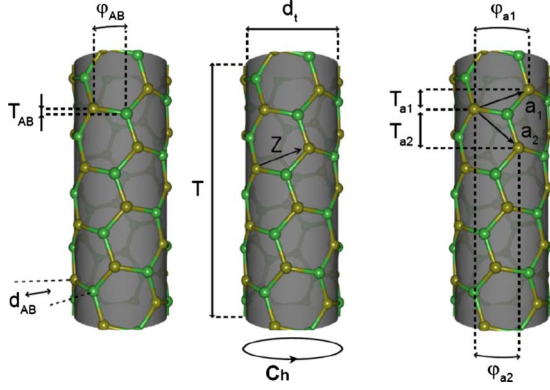


FIG. 1. (Color online) Unit cell of a (4,2) carbon nanotube showing its structural parameters. The distance between the AB atoms in the nanotube unit cell and the graphene lattice vectors \mathbf{a}_1 and \mathbf{a}_2 projected on the nanotube cylindrical surface are decomposed into their components along the axial, (T_{AB} , T_{a1} , and T_{a2}) and circumferential directions (φ_{AB} , φ_{a1} , and φ_{a2}) (Ref. 13).

momentum of the tube in the axial direction.¹¹ A torsion τ causes a variation in the graphene primitive vectors, such that $\Delta\varphi_{a1} = \tau T_{a1}$ and $\Delta\varphi_{a2} = \tau T_{a2}$, where φ_{a1} and φ_{a2} are the components of the primitive vectors of graphene in the circumferential direction (see Fig. 1), and T_{a1} and T_{a2} are their components along the axial direction. For a nanotube of length L and diameter d_t , the torsion angle (ϕ_τ) can be calculated (in radians) as $\phi_\tau = 2\tau L/d_t$.

The carbon-nanotube electronic bands were calculated using an extended tight-binding model considering the DFT-based parametrization.¹² The Brillouin zone (BZ) defined by the helical-angular construction of the nanotube¹¹ can be understood in terms of d cutting lines separated by $2/d_t$ on the direction perpendicular to the nanotube axis. The length of the BZ is $2\pi N/(Td)$, where N is the number of hexagons in the nanotube translation unit cell and $d = \text{gcd}(n, m)$, where gcd stands for the greatest common divisor. The electronic contribution to the total energy (E) is calculated by integrating the band structure along this extended BZ. The contribution of the interatomic repulsion to the total energy is also obtained from the work of Porezag *et al.*¹²

To illustrate the torsion effect on E for some sample SWNTs, we first relaxed the nanotube structure for fixed values of torsion. The other structural parameters which were allowed to relax are shown in Fig. 1: longitudinal length of the SWNT unit cell (T), nanotube diameter (d_t), and the axial and angular distances between the A and B carbon atoms (T_{AB} and φ_{AB}). The dependence of the total energy E on the torsion τ can be seen in Fig. 2(a) for an (8,0) zigzag (solid blue circles) and a (5,3) chiral nanotube (red triangles). A clear parabolic behavior can be seen for both nanotubes. However, it can also be observed that while for the zigzag nanotube the energy minimum is at $\tau=0$, for the chiral nanotube, the most stable configuration occurs for $\tau \neq 0$, which indicates that chiral nanotubes have a natural torsion τ_0 . The magnitude of this natural torsion $\tau_0 = 0.0127 \text{ nm}^{-1}$ is equivalent to twisting the nanotube of 2π every 137 nm of its length (or twisting a 1- μm -long nanotube 7.3 times).

This natural torsion can be understood within the frame-

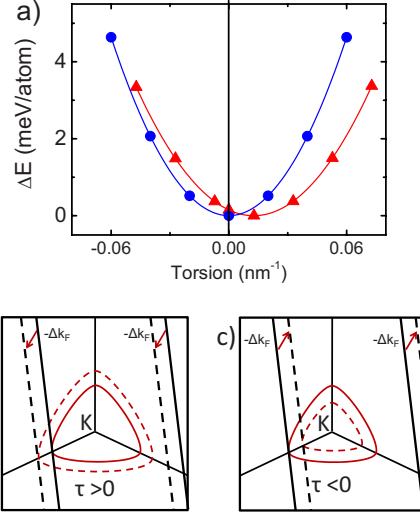


FIG. 2. (Color online) Variation in the total energy with the applied torsion for an (8,0) nanotube (blue circles) and a (5,3) nanotube (red triangles). (a) The solid line represents a parabolic fit. [(b) and (c)] Sketch of the graphene reciprocal space near the K point (\mathbf{k}_F). Two nearest cutting lines for undeformed (5,3) nanotube are shown as solid lines. For torsioned nanotubes the cutting lines, which are shifted by $-\Delta\mathbf{k}_F$ as an effect of torsion, are shown as dashed lines. The value of $\Delta\mathbf{k}_F$ has an opposite direction for (b) positive torsion and (c) negative torsion. In (b) the torsion shifts the cutting line nearest to K away from the K point while in (c) the torsion shifts it toward the K point. The equienergy contour for each of the cutting lines nearest to K in (b) and (c) are also shown.

work of the zone folding of the electronic states of graphene due to the boundary conditions imposed by the curvature of the nanotube. The effects of torsion on the electronic bands of carbon nanotubes were investigated by Yang and Han¹ using a Hückel tight-binding model. Within this simple approach, the torsion effects are estimated in terms of a shift Δk_F of the Fermi point, \mathbf{k}_F , (point where the graphene valence and conduction bands touch each other), also known as the Dirac point, with respect to the cutting lines defined by the allowed wave vectors in the graphene reciprocal space. The direction and magnitude of the shift are given by

$$\Delta\mathbf{k}_F = \frac{\sqrt{3}d_t}{2a}\tau \sin(3\theta)\hat{\mathbf{e}}_c + \frac{\sqrt{3}d_t}{2a}\tau \cos(3\theta)\hat{\mathbf{e}}_t, \quad (1)$$

where θ is the nanotube chiral angle and $a = \sqrt{3}a_{cc}$, in which $a_{cc} \sim 0.142 \text{ nm}$ is the distance between the A and B atoms in graphene. The unit vectors $\hat{\mathbf{e}}_c$ and $\hat{\mathbf{e}}_t$ are aligned along the circumferential and translational directions, respectively. This model was able to predict the behavior of the gap in metallic nanotubes with applied torsion.¹

In this sense, the torsion will cause a change in the relative position (by $-\Delta\mathbf{k}_F$) of the cutting lines with respect to the Fermi point, keeping both the distance between the cutting lines and their length unchanged. To illustrate this effect on the total electronic energy, Figs. 2(b) and 2(c) depict two cutting lines which pass near the \mathbf{k}_F point for an untorsioned (5,3) semiconducting nanotube (solid lines) and for positively and negatively torsioned tubes, given by dashed lines

in (b) and (c), respectively. For clarity, the cutting lines were moved by $-\Delta\mathbf{k}_F$ while the position of the Fermi point was kept constant. In this particular case, for a positive torsion, the cutting line which is closer to the K point (\mathbf{k}_F) moves away from the Fermi point causing the valence band to shift down in energy. On the other hand, for a negative torsion, this cutting line moves toward the K point and thus the electronic energy shifts up. For other cutting lines farther away from the \mathbf{k}_F point, the behavior can either be similar or opposite to this, depending on whether the cutting line passes by one side or the other of the nearest \mathbf{k}_F point. For large diameter nanotubes, this alternation tends to cancel out this effect so that the influence of a torsional stress on the total energy decreases rapidly. However, for small diameter tubes, the cutting lines which are closer to the \mathbf{k}_F point, where the electronic dispersion is large, will contribute the most to the change in the total energy due to torsion.

The origin of the natural torsion can be understood by noting that in the case of the nanotube depicted in Figs. 2(b) and 2(c), the derivative of the total energy with respect to the torsion ($\partial E/\partial\tau$) does not vanish for $\tau=0$. Although this fact can be directly inferred from the work of Yang and Han,¹ the authors did not perceive that a natural torsion would be a direct consequence of their findings: this nonvanishing derivative can be interpreted as a residual torque which causes the nanotube to deform itself in order to find a lower-energy configuration and gives rise to a natural torsion. Although this process is in some way similar to the underlying physics behind the Peierls instability in one-dimensional metals, which has been previously investigated for SWNTs,¹⁵ this torsion is not an effect of such lattice instabilities originating from a strong electron-phonon coupling. An important confirmation of this is the fact that neither the armchair SWNT nor the metallic zigzag SWNT, for which the electron-phonon interaction should be large, is naturally torsioned. Instead, the natural torsion is associated with the lack of an inversion symmetry, which is present for a graphene sheet, in the chiral SWNT structure.

To better understand the dependence of the natural torsion on the SWNT diameter, we can use some basic results from continuum elasticity theory. Within that approach, a torsion (τ) caused by a given torque Y can be calculated as $\tau = Y/GJ$, where G is the shear modulus of the material and J is the torsion constant, or the polar moment of inertia (in the case of cylindrical cross sections). For a hollow tube, the value of J is given by

$$J = \frac{\pi}{2}(R_{\text{out}}^4 - R_{\text{in}}^4) \sim 2\pi R^3 \Delta R, \quad (2)$$

where R_{in} and R_{out} are the inner and outer radii of the tube, and R and ΔR are the mean radius and the width of the tube wall. This last approximation is only valid when the wall width is much smaller than the radius and thus should apply only for large diameter nanotubes. We thus conclude that if the torque is independent of the nanotube diameter, a $1/d_i^3$ behavior should be expected for the natural torsion in larger diameter carbon nanotubes.

To investigate the dependence of the natural torsion on the nanotube diameter and chirality, the torsion was also allowed

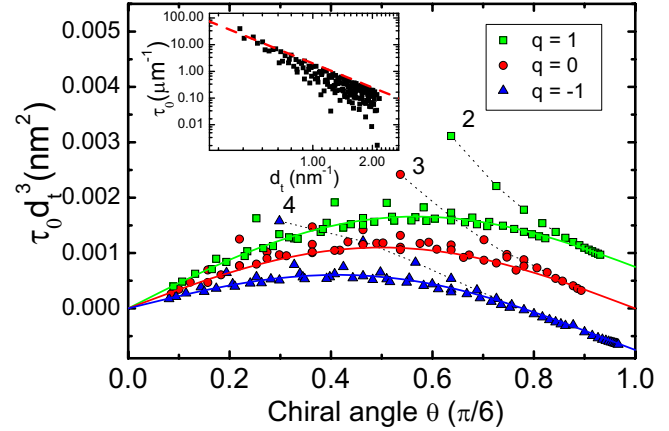


FIG. 3. (Color online) Dependence of $\tau_0 d_i^3$ on the chiral angle (θ , in units of $\pi/6$) for the different $\text{mod}(2n+m, 3)=q$ families, $q = 0, -1$, and 1 . The solid lines show the curves given by Eq. (3). The inset shows the dependence of the natural torsion on the nanotube diameter on a logarithmic scale. The dashed line in the inset is a guide to the eye given by the equation $\tau_0 = A d_i^{-3}$, where $A = 2 \times 10^{-3} \text{ nm}^2$.

to relax. The structural relaxation was performed in a configuration space of five parameters (τ , φ_{AB} , T_{AB} , T , and d_i) using the conjugate gradients method with a convergence threshold for the total energy of 10^{-8} meV. It should be mentioned that the remaining parameters T_{a1} , T_{a2} , ϕ_{a1} , and ϕ_{a2} are constrained by the nanotube structure, being thus determined by the values of T and τ . In the inset to Fig. 3, the dependence of the natural torsion on nanotube diameter can be observed (each point in the figure represents a nanotube with a diameter between 0.5 and 1.76 nm) on a logarithmic scale. A dashed line is shown in the inset to Fig. 3 as a guide to the eye representing the $\tau_0 = A d_i^{-3}$, with $A = 2 \times 10^{-3} \text{ nm}^2$, behavior obtained from the continuum theory. Note that this line corresponds to a limiting behavior. The fact that in the limit of large diameter carbon nanotubes the behavior falls into a $1/d_i^3$ dependence indicates that the amount of torque given by the nanotube electronic structure to the lattice is not further decreasing with increasing nanotube diameter. For smaller diameter nanotubes, the dependence of the natural torsion on the nanotube diameter deviates from this behavior, indicating that for these nanotubes the amount of torque originating from the electronic structure is dependent of the nanotube diameter. This effect originates from the increasing overlap between the π and σ bands due to the curvature-induced rehybridization. Also, the effects of higher-order terms in J should contribute to this deviation.

The dependence of the natural torsion on the chiral angle can be more clearly investigated if the $1/d_i^3$ dependence of τ_0 on d_i is removed by plotting $\tau_0 d_i^3$ as a function of chiral angle θ , as shown in Fig. 3. Note that most of the nanotubes follow either one of three specific behaviors, which are shown in different colors (online) and symbols. These nanotubes correspond to the different $\text{mod}(2n+m, 3)=q$ values with q being equal 0 for metallic single-wall carbon nanotubes (M-SWNTs) and 1 or -1 for semiconducting single-wall carbon nanotubes (S-SWNTs). It is important to mention that, as

discussed above, for the smallest diameter nanotubes τ_0 does not behave with a $1/d_t^3$ dependence, and thus multiplying τ_0 by d_t^3 does not completely remove its diameter dependence. For clarity, the nanotubes in families $2n+m=2, 3$, and 4 for which the deviation is the greatest are highlighted by dotted lines in Fig. 3. For the M-SWNTs (shown in red circles), the value of $\tau_0 d_t^3$ follows a $\sin(6\theta)$ behavior, which leads to a zero natural torsion for both limiting values of θ , namely, 0 and $\pi/6$, corresponding to zigzag and armchair nanotubes, respectively. This result is expected since these nanotubes have a reflection plane along the nanotube axis, which guarantees that the effect of torsioning the nanotube is the same for either direction and thus the total energy (E) has to have an extremum for $\tau=0$. However, for the S-SWNTs, shown in green squares and blue triangles, near the $\theta \sim \pi/6$ region the behavior is different from the simple $\sin(6\theta)$ function and also different for $q=1$ and -1 . This interesting behavior can be well described by adding a term which depends on $\sin(3\theta)$. The main chiral angle dependence of the natural torsion could then be well described by the following equation:

$$\tau_0 d_t^3 = a \sin(6\theta) + qb \sin(3\theta) \quad (3)$$

with $a \sim 1.1 \times 10^{-3} \text{ nm}^2$ and $b \sim 0.75 \times 10^{-3} \text{ nm}^2$, and $q=1, -1$, and 0 depending on the nanotube family, as explained above. It can thus be seen that for near-armchair $q=-1$ S-SWNTs, the natural torsion turns out to be in the opposite direction of the chirality of the nanotube (defined as the angle between the chiral vector and the graphene lattice vector \mathbf{a}_1), whereas for the majority of the nanotubes the natural torsion goes in the same direction as the nanotube chirality.

It is important here to comment that for short nanotubes the finite size of the nanotube can affect the value of the natural torsion. Finite-size effects were not taken into account in the present study, for which only the intrinsic natural torsion effects are investigated. We can estimate for which range of nanotube lengths the calculations performed here are valid by observing that resonance Raman scattering experiments in DNA-wrapped nanotubes indicate that for nanotubes longer than 100 nm the electronic and vibrational properties of the nanotubes are not affected by their finite size.¹⁶ In fact, since the driving force for the emergence of the natural torsion comes from the electronic structure while loose nanotube ends allow for an extra relaxation of the electronically driven torque, we should expect that the natural torsion will increase with decreasing nanotube length. In this sense, for nanotubes longer than 100 nm, the natural torsion calculated in this work should be regarded as a lower limit. For shorter nanotubes, the finite size of the nanotube will affect its electronic properties, thus affecting the natural torsion. A more detailed study of the finite-size effects is very important for shorter nanotubes and should be the subject of further investigation.

Another matter of great importance is the question of whether the presence of a natural torsion can produce measurable effects at room temperature or if this effect can only be probed at very low temperatures. In this sense, we should point out that although for most nanotubes the energy difference between the torsioned and untorsioned configurations is

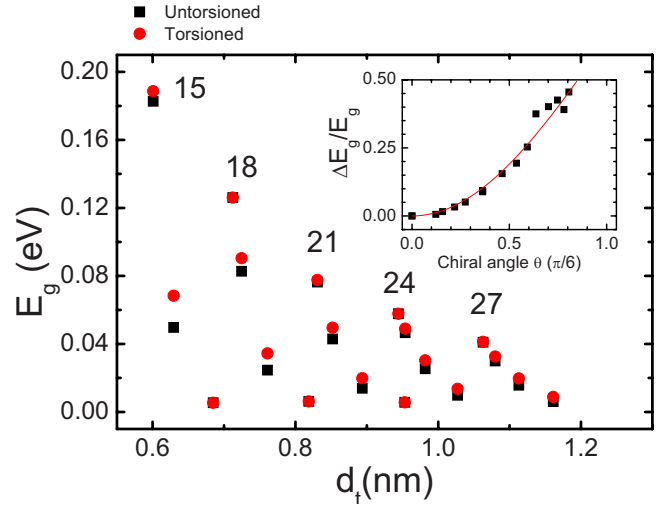


FIG. 4. (Color online) Dependence of the minigap in untorsioned (black square box) and torsioned (red circle) metallic nanotubes on the nanotube diameter. The numbers indicate the $2n+m$ families. The inset shows the θ dependence of the relative change in the minigap for the nanotubes in the main figure. The chiral angle is written in units of $\pi/6$. The solid line in the inset represents a curve given by $\Delta E_g/E_g = 0.65[1 - \cos(3\theta)]$.

lower than 0.1 eV/atom, see Fig. 2(a), the natural torsion should affect the nanotube properties at much higher temperatures since the nanotube properties will be determined by the average nanotube torsion, which is different from zero, independent of the temperature.

The presence of this natural torsion has several important implications upon nanotube science. For example, in the calculation of excitonic effects, only electronic states within a single cutting line are taken into account for the evaluation of each excitonic state. This approximation has been explained by the fact that the excitonic wave function around the nanotube axis is delocalized and thus a single angular momentum state can be used to describe it.¹⁷ This remains true for naturally torsioned nanotubes. However, only pure angular-momentum-related quantum numbers are good quantum numbers for torsioned nanotubes. These pure angular momenta define a number d of different cutting lines according to a helical-angular representation of the nanotube structure.¹¹ In fact, since torsioned nanotubes do not have a pure translational symmetry, in principle, all group theoretical analysis based on the group of the wave vector¹¹ will not be strictly valid for torsioned nanotubes and the line group analysis developed by Damnjanović *et al.*¹⁸ should be applied. Further group theoretical investigation is needed in order to understand what are the actual effects of this symmetry breaking to the symmetry-related properties. One of the most relevant effects of this natural torsion is on the electronic transition energies and these effects may be responsible for discrepancies between previous theoretical calculations and experimental results in SWNTs. For example, our calculations show an upshift on the order of 64 meV for the E_{11} transition of a naturally torsioned (4,2) nanotube when compared to its undeformed structure. Also, as shown in Fig. 4, the natural torsion has a strong effect on the mag-

nitude of the minigap present in $\text{mod}(2n+m,3)=0$ nanotubes. These minigaps are observed to increase by as much as 50% due to the natural torsion. Also, our calculations predict that the increase in the minigap is independent of the nanotube diameter and scales as $1-\cos(3\theta)$ (except for the armchair nanotubes, for which there is no torsion-induced gap). Also, at a more conceptual level, the presence of this torsion implies a revision of the definition of the chiral angle since it can no longer be calculated from intrinsically structural properties, such as the (n,m) values for the nanotube and is dependent on the nanotube electronic structure and its effect on the value of the natural torsion.

In summary, we have used an extended tight-binding approach to investigate the natural torsion in small diameter chiral single-wall carbon nanotubes. The presence of this natural torsion can be attributed to a torsional instability originating from the lack of an inversion symmetry of the chiral nanotubes by their helical structure and can be traced back to the properties of graphene ribbons by considering a simple zone-folding technique.¹⁹ The calculated natural torsion was shown to decrease with $1/d_i^3$ and for metallic nanotubes a dependence on $\sin(6\theta)$ was found, with a maximum

torsion for a chiral angle $\theta=\pi/12=15^\circ$. For semiconducting nanotubes, the behavior is slightly changed and a term depending on $\sin(3\theta)$ needs to be added or subtracted (depending on the nanotube family) to take into account the asymmetry of the electronic-band structure near the K point of graphene. The presence of this natural torsion has several important implications on the physics of nanotubes: it causes a further opening of the minigaps in metallic SWNTs, changes the optical transition energies and also has implications on the breaking of the pure translational symmetry of the chiral nanotubes.

E.B.B. Acknowledges NSF-CNPq (Grant No. 491083/2005-0) joint collaboration, CNPq under Grant No. 550435/2007-7 and Funcap for financial support. M.S.D. acknowledges NSF under Grant No. DMR 07-04197. R.S. acknowledges MEXT under Grant No. 20241023. A.G.S.F. acknowledges partial support from CNPq Grants No. 577489/2008-9, No. 477392/2007-5, No. 306335/2007-7 and Rede Nacional de Pesquisa em Nanotubos de Carbono (MCT-CNPq).

*ebarros@fisica.ufc.br

¹Liu Yang and Jie Han, *Phys. Rev. Lett.* **85**, 154 (2000).

²S. B. Cronin, A. K. Swan, M. S. Ünlü, B. B. Goldberg, M. S. Dresselhaus, and M. Tinkham, *Phys. Rev. Lett.* **93**, 167401 (2004).

³S. B. Cronin, A. K. Swan, M. S. Ünlü, B. B. Goldberg, M. S. Dresselhaus, and M. Tinkham, *Phys. Rev. B* **72**, 035425 (2005).

⁴R. B. Capaz, C. D. Spataru, P. Tangney, M. L. Cohen, and S. G. Louie, *Phys. Status Solidi B* **241**, 3352 (2004).

⁵S. J. Papadakis, A. R. Hall, P. A. Williams, L. Vicci, M. R. Falvo, R. Superfine, and S. Washburn, *Phys. Rev. Lett.* **93**, 146101 (2004).

⁶A. M. Fennimore, *Nature (London)* **424**, 408 (2003).

⁷Y. N. Gartstein, A. A. Zakhidov, and R. H. Baughman, *Phys. Rev. B* **68**, 115415 (2003).

⁸J. R. Xiao, B. A. Gama, and J. W. Gillespie, Jr., *Int. J. Solids Struct.* **42**, 3075 (2005).

⁹H. Liang and M. Upmanyu, *Phys. Rev. Lett.* **96**, 165501 (2006).

¹⁰T. Chang, *Appl. Phys. Lett.* **90**, 201910 (2007).

¹¹E. B. Barros, A. Jorio, Ge. G. Samsonidze, R. B. Capaz, A. G. Souza Filho, J. Mendez Filho, G. Dresselhaus, and M. S.

Dresselhaus, *Phys. Rep.* **431**, 261 (2006).

¹²D. Porezag, Th. Frauenheim, Th. Köhler, G. Seifert, and R. Kaschner, *Phys. Rev. B* **51**, 12947 (1995).

¹³G. Samsonidze, Ph.D. thesis, Massachusetts Institute of Technology, 2006.

¹⁴H. M. Lawler, J. W. Mintmire, and C. T. White, *Phys. Rev. B* **74**, 125415 (2006).

¹⁵N. A. Viet, H. Ajiki, and T. Ando, *J. Phys. Soc. Jpn.* **63**, 3036 (1994).

¹⁶S. G. Chou, H. Son, M. Zheng, R. Saito, A. Jorio, J. Kong, G. Dresselhaus, and M. S. Dresselhaus, *Chem. Phys. Lett.* **443**, 328 (2007).

¹⁷J. Jiang, R. Saito, Ge. G. Samsonidze, A. Jorio, S. G. Chou, G. Dresselhaus, and M. S. Dresselhaus, *Phys. Rev. B* **75**, 035407 (2007).

¹⁸M. Damnjanović, I. Milosević, T. Vuković, and R. Sredanović, *Phys. Rev. B* **60**, 2728 (1999).

¹⁹R. Saito, G. Dresselhaus, and M. S. Dresselhaus, *Physical Properties of Carbon Nanotubes* (Imperial College Press, London, 1998).